

# A Merger Tree with Microsolar Mass Resolution: Application to $\gamma$ -ray Emission from Subhalo Population

Carlo Giocoli<sup>1,2,3</sup>, Lidia Pieri<sup>1,4,5</sup>, Giuseppe Tormen<sup>1</sup> and Jorge Moreno<sup>6</sup>  $\star$

<sup>1</sup> *Dipartimento di Astronomia, Università degli Studi di Padova, Vicolo dell'osservatorio 2 I-35122 Padova, Italy*

<sup>2</sup> *Istituto Nazionale di Astrofisica - Osservatorio Astronomico di Padova, Vicolo dell'osservatorio 2 I-35122 Padova, Italy*

<sup>3</sup> *Zentrum für Astronomie, ITA, Universität Heidelberg, Albert-Ueberle-Str. 2, 69120 Heidelberg, Germany*

<sup>4</sup> *Consorzio Interuniversitario di Fisica Spaziale, Villa Gualino, Viale Settimio Severo, 63, I-10133 Torino, Italy*

<sup>5</sup> *Istituto Nazionale di Fisica Nucleare - Sezione di Padova, Via Marzolo 8 I-35131 Padova, Italy*

<sup>6</sup> *Department of Physics & Astronomy, Haverford College, 370 Lancaster Avenue, Haverford, PA 19041, USA*

## ABSTRACT

The hierarchical growth of dark matter haloes, in which galaxies are hosted, has been studied and modeled using various approaches. In this paper we use a modified version of the Sheth & Lemson algorithm for a  $\Lambda$  cold dark matter power spectrum, and model the growth of a Milky-Way sized halo with microsolar mass resolution, corresponding to the typical Jeans mass for a dark matter Weakly Interacting Massive Particle with mass of 100 GeV. We then compute the *unevolved* subhalo mass function and build-up a Milky-Way halo placing and evolving its satellites. This subhalo population is used to study the  $\gamma$ -ray emission from dark matter annihilation. In this case, the subhaloes which populate the host halo have been computed considering only progenitor haloes accreted by the main branch of the tree, so as to correctly treat the embedding of sub-subhaloes inside subhaloes. Each subhalo will indeed host at the present-time sub-subhaloes accreted when it was an isolated system. In order to compute the sub-subhalo population of a Milky-Way dwarf galaxy, like Draco, and to study its  $\gamma$ -ray emission, we first estimate the Draco virial mass at merging redshift  $z_m$  and then we run the merger tree from  $z_m$  following the halo down to the dark matter Jeans mass. We then study the effect on the Fermi-LAT (GLAST) detectability for both subhaloes in the Milky-Way and in Draco, and we show how subhaloes cannot be responsible for the boost factor needed for detection.

**Key words:** galaxies: halo - cosmology: theory - dark matter - methods: analytical, numerical

## 1 INTRODUCTION

In the standard scenario of structure formation galaxies reside in massive Dark Matter (DM) haloes, where baryons can shock, cool and eventually form stars. Haloes form by gravitational instability, starting from some density fluctuation field  $\delta(\vec{x})$ . Specifically, a dark matter halo with mass  $M \propto R^3$ , forms when the linear density field, smoothed on scale  $R$ , exceeds some critical threshold  $\delta_c$  (Bond et al. 1991; Carroll et al. 1992; Lacey & Cole 1993; Eke et al. 1996).

In a Cold Dark Matter (CDM) framework, the galaxy formation process is hierarchical along cosmic time: small systems collapse earlier, in a denser universe, and later merge to form larger haloes. In particular, haloes often grow as a consequence of repeated merging events

with smaller satellites. Present-day surviving satellites form the so-called subhalo (or substructure) population of a given host system (Moore et al. 1999; Springel et al. 2001; Gao et al. 2004; van den Bosch et al. 2005; Giocoli et al. 2008a; Zentner et al. 2005).

Dark matter haloes and subhaloes provide the environment in which galaxies form and evolve (Bullock et al. 2000; Somerville 2002; Kravtsov et al. 2004; Vale & Ostriker 2006). Therefore, understanding the assembly histories of dark matter haloes is the first step towards the comprehension of the more complex processes involved in galaxy formation.

In order to study the framework of structure formation, two different approaches have commonly been used. The first is to run  $N$ -body simulations (Springel et al. 2001, 2005; Diemand et al. 2007a,b). These are very powerful tools, that can be used to reproduce the collapse of dark matter haloes with high mass and force resolution, both on galaxy and

$\star$  Email: cgiocoli@ita-uni-heidelberg.de, pieri@iap.fr, giuseppe.tormen@unipd.it, jmoreno@haverford.edu.

galaxy-cluster scales. They allow to follow gravitational collapse up to its fully non-linear evolution. On the other hand, simulations are computationally expensive, and nonetheless cannot cover the full spectrum of masses relevant to structure formation. The second approach is to use some analytical modeling, which allows a detailed study of the merging history of haloes over an arbitrarily large mass range, under suitable simplification of the problem. This is the case of the Press & Schechter formalism (Lacey & Cole 1993; Sheth 1998; Sheth & Lemson 1999; Sheth 2003).

As underlined before, haloes collapse on a certain scale once the linear density contrast smoothed on that scale exceeds some threshold value. The nonlinearities introduced by these virialized objects do not affect the collapse of overdense regions on larger scales. This simple assumption leads to the derivation of the global mass function of dark matter haloes that is in fair agreement with that found in  $N$ -body simulations (Lacey & Cole 1993; Somerville et al. 2000; Sheth & Tormen 1999, 2002). During the last decades, an extension of this theory was made by several authors (Lacey & Cole 1993; Bond et al. 1991; Bower 1991) with the aim of computing the probability that a halo of mass  $m$ , at redshift  $z$ , belongs to a given halo of mass  $M_0$  at redshift  $z_0 < z$  (Lacey & Cole 1993; Sheth & Tormen 2002). This quantity was named “conditional” or “progenitor” mass function,  $f(m, z|M_0, z_0)dm$ . This allowed different authors to estimate quantities such as the merger (Neistein & Dekel 2008) and creation rate (Percival & Miller 1999; Percival et al. 2000; Moreno et al. 2007), and the formation time distribution of dark matter haloes (Sheth & Tormen 2004; Giocoli et al. 2007).

The extended Press-Schechter formalism can be numerically implemented to produce stochastic realizations of the merging history tree of haloes of any mass; these Monte Carlo merging histories can have, theoretically, arbitrary resolution in mass and time, and their result is the full population of progenitor haloes at all times, for some final halo. The only thing they do not provide is spatial information on the haloes themselves. Therefore, when the focus is on the statistical properties of haloes and not on their position or internal structure, Monte Carlo merger trees have the advantage - over  $N$ -body simulation - of virtually unlimited mass resolution. Implementing a code to reach the required resolution is however not straightforward, and caution must be used in order to preserve consistently with the theory.

In this paper we will build a spherical collapse Monte Carlo merger tree with arbitrary mass and time-step resolution, and will consider a  $\Lambda$ CDM-power spectrum. We will populate a Milky-Way sized halo with subhaloes with masses as small as  $10^{-6}M_\odot$ . This value correspond to the typical Jeans mass for the a CDM Weakly Interacting Massive Particle (WIMP) particle with  $m_{\text{DM}} = 100\text{GeV}$  (Green et al. 2004, 2005). Such a value for the minimum mass can actually vary between  $10^{-12}$  and  $10^{-4}M_\odot$  depending on the underlying particle physics (Profumo et al. 2006).

We will take into account the progenitor haloes accreted by the main branch of our Milky-Way like halo, in order to obtain a snapshot of the spatial distribution of substructures today. **In this way we will select only the first order of substructures which populate the halo today (those which are orbiting in the host halo potential), in order to correctly model the radial dependence**

**of subhalo properties. In other words, we will avoid the bias of our previous works (see, e.g. Giocoli et al. (2008b)) towards the small scale structures. In those works, the embedding of sub-subhalos within subhalos was not treated correctly. Each structure existing inside the main halo was indeed considered as orbiting inside the potential of the host halo itself. In this way, an analytical treatment of the effect of subhalos on the expected photon flux from DM annihilation was possible. However, it was not possible to take into consideration the fact that a number of small scale structures are indeed sub-substructures, that is to say they are orbiting inside the potential of the subhalo they belong to, and not inside the potential of the host halo. In the present work we will be able to separate and study the effect of introducing sub-subhalos.** With the same partition code we will thus compute the subhalo population of subhaloes (i.e. subhaloes within subhaloes), and we will consider the special case of a Draco-like satellite. In the second part of the paper we will estimate the  $\gamma$ -ray emission from dark matter annihilation, in the subhalo population of the Milky-Way and of a Draco-like subhalo, and will discuss the different contributions to  $\gamma$ -ray emissions due to the smooth and clumpy components of the considered systems.

The paper is organized as follows: in Sec. 2 we describe the merger tree technique developed by (Sheth & Lemson 1999) and its generalization to a  $\Lambda$ CDM power spectrum. Sec. 3 is dedicated to the study of the merger tree of a Milky-Way sized halo, and to compute its mass accretion history along cosmic time and its satellite mass function. In Sec. 4 we model the hierarchical growth of a sample of Draco-like satellites until their merging time with the main Milky-Way progenitor halo. In Sec. 5 we study the  $\gamma$ -ray emission from dark matter annihilation in subhaloes and sub-subhaloes and estimate the possibility to be detected with the Fermi-LAT telescope. In Sec. 6 we discuss our results and conclude.

## 2 METHOD AND MERGER TREE

The simplest algorithm for a merger tree uses a binary split. In this scenario each halo is split in two haloes at an earlier epoch. Each of these is in turn divided in other two pieces, and so on until all halo masses fall below an arbitrary chosen and desired mass resolution  $m_\epsilon$  (Lacey & Cole 1993; Cole & Kaiser 1988; Cole 1991; Kauffmann & White 1993). However, Somerville & Kolatt (1999) showed the failure of using a binary merger tree. In this way the first halo which is chosen from the Press & Schechter distribution follows the correct probability, but the second one is chosen only in order to conserve mass and does not follow the theoretical model as expected. This leads to a conditional mass function and formation redshift distribution in disagreement with the extended Press & Schechter predictions. To solve this problem, Somerville & Kolatt (1999) proposed a new algorithm able to reproduce the conditional mass function quite well, at the expenses of using a finely tuned grid of time-steps.

On the other hand, Sheth & Lemson (1999) used the results of Sheth (1996) and realized that, for white-noise initial conditions, mutually disconnected regions are mutu-

ally independent. In this case it is possible to split a halo into progenitors very efficiently. The so obtained conditional mass function is in excellent agreement with the theoretical model of the spherical collapse. The great advantage of this method is that it is possible to obtain arbitrary high mass resolution for any given time-step, generating progenitors in a very fast and efficient way.

In this section we will describe the way the method developed by Sheth & Lemson (1999) can be generalized considering a  $\Lambda$ CDM power spectrum. Using this algorithm, we will follow the creation and the assembly history of a present-day Milky-Way sized halo.

Assuming that the dark matter is a WIMP, the Jeans mass of the smaller DM halo is given by its free-streaming scale (Green et al. 2004, 2005), and for a DM particle mass of 100 GeV this smallest halo mass has a typical mass  $m_J = 10^{-6} M_\odot$ . We therefore extend our merger tree down to microsolar mass resolution, in order to study the present-day subhalo population down to the dark matter Jeans mass.

## 2.1 Poissonian Distribution and Gaussian Initial Conditions

Let us start considering an initial Poissonian distribution of identical particles. Epstein (1983) and Sheth (1995) showed that the probability to find a clump containing  $N$  particles is expressed by the Borel distribution (Borel E. 1942):

$$\eta(N, b) = \frac{(Nb)^{N-1} e^{-Nb}}{N!}, \quad (1)$$

where the variables  $N$  and  $b$  are such that  $N \geq 1$  and  $0 \leq b < 1$ . Sheth (1995) also showed that this equation can be extended to the continuous case, in order to describe dark matter halo clustering. In this case the variable  $b$  has a redshift dependence given by:

$$b = 1/(1 + \delta_c(z)).$$

where  $\delta_c(z)$  is the critical overdensity threshold predicted by the spherical collapse model, decreasing as the universe expands. The probability that a randomly chosen particle belongs to an  $N$ -clump is given by  $f(N, b) = (1-b)N\eta(N, b)$ . For large values of  $N$  and small values of  $\delta_c$ , the factorial Stirling's approximation gives:

$$\begin{aligned} f(N, \delta_c) &= \frac{\delta_c}{(1 + \delta_c)} \left( \frac{N}{1 + \delta_c} \right)^{N-1} \frac{e^{-N/(1 + \delta_c)}}{(N-1)!} \\ &\rightarrow \frac{\delta_c}{\sqrt{2\pi N}} \exp\left(-\frac{N\delta_c^2}{2}\right). \end{aligned} \quad (2)$$

Since all matter is in clumps, it holds the relation  $\sum_{N=1}^{\infty} f(N, \delta_c) = 1$ . Sheth (1995) showed also that Eq. (2) can be obtained starting from an initial Gaussian density field with white noise initial conditions ( $P(k) \sim k^n$  with  $n = 0$ ). This equivalence underlines that the Poissonian distribution can be thought as the analogue discrete of the white noise Gaussian power spectrum (Bond et al. 1991; Lacey & Cole 1993, 1994).

The critical collapse overdensity decreases with the expansion of the universe, so that small systems collapse earlier than large ones, i.e., dark matter halo clustering progresses hierarchically. An important quantity that describes the hierarchical growth of the haloes is the conditional distribution. It gives the probability that a particle, belonging to a

clump with  $N$  particles at time  $b_0$ , is part of an  $n$ -clump at  $b_1 < b_0$ , and can be written as:

$$\begin{aligned} f(n, b_1|N, b_0) &= N \left(1 - \frac{b_1}{b_0}\right) \binom{N}{n} \frac{n^n}{N^N} \\ &\times \left(\frac{b_1}{b_0}\right)^{n-1} \left[N - n\frac{b_1}{b_0}\right]^{N-n-1}, \end{aligned} \quad (3)$$

where  $1 \leq n \leq N$  and  $0 \leq b_1/b_0 \leq 1$  (Sheth 1995).

However, for a complete description of the merging history tree of an  $N$ -clump at  $b_0$ , we also need to know the probability that, at  $b_1$ , it is divided in a sample of  $n_j$   $j$ -clumps with  $k$  subfamilies (so that  $n_1 + \dots + n_N = k$ ). Recalling the conservation of the particle number,  $\sum_{j=1}^k j n_j = N$ , the Poissonian Galton-Watson branching process gives the following equation for this probability:

$$\begin{aligned} p(n_1, \dots, n_k, b_1|N, b_0) &= \frac{[N(b_1 - b_0)]^{n-1} e^{-N(b_1 - b_0)}}{\eta(N, b_0)} \\ &\times \prod_{j=1}^k \frac{\eta(j, b_1)^{n_j}}{n_j!}, \end{aligned} \quad (4)$$

where  $\eta(l, b)$  is the Borel distribution with time parameter  $b$  (see Sheth (1996) for more details). Since  $b_0$  can be related to a density, the volume of the  $N$ -clump can be written as:

$$V_{N,0} = \frac{N}{\bar{n}(1 + \delta_{c,0})}, \quad (5)$$

where  $\bar{n}$  denotes the average density of the universe. Eq. (4) can be thought of as the probability that a region with  $N$  particles, having density  $\bar{n}(1 + \delta_{c,0})$ , contains  $k$  subregions each at average density  $\bar{n}(1 + \delta_{c,1})$ , where  $\delta_{c,1} \geq \delta_{c,0}$ .

The merging history of a present-day halo is described using the Extended-Press & Schechter formalism (Lacey & Cole 1993) and formulated in terms of its conditional mass function along consecutive time steps. Let us now consider an  $n$ -subclump of the  $N$ -clump, at time  $b_1$ ; in Appendix A of Sheth & Lemson (1999) it is shown that, if  $V_{n,1} = n/\bar{n}(1 + \delta_{c,1})$  is its associated volume, the remaining particles  $N - n$  will occupy a volume such that:

$$\frac{N - n}{V_{N,0} - V_{n,1}} \equiv \bar{n}(1 + \delta'_c) = \frac{\bar{n}}{b'}, \quad (6)$$

where  $b'/(1 + \delta'_c)$  is the unknown quantity to be determined and represents the density in the volume  $V_{N-n}$ .

The spherical collapse model predicts that a group of uncollisionless  $N$  particles, with the same mass  $m_{\text{DM}}$ , collapses forming a dark matter  $M$ -halo ( $M = N \times m_{\text{DM}}$ ), if the smoothed density fluctuation filed on scale  $R \sim M^{1/3}$  exceeds its predicted critical virial value (Eke et al. 1996). For each collapsed system we can define its associated mass variance as:

$$S(M) = \frac{1}{(2\pi)^3 V_R} \int d^3k \langle |\hat{\delta}(k)|^2 \rangle \hat{W}^2(kR), \quad (7)$$

where  $\hat{W}(kR)$  and  $\hat{\delta}(k)$  represent respectively the Fourier transform of the smoothing window function and of the density fluctuation field.

It is possible to show that in the continuous limit Eq.s (1) and (4) give:

$$f(\nu)d\nu = 2\sqrt{\frac{1}{2\pi}} e^{-\nu^2/2} d\nu. \quad (8)$$

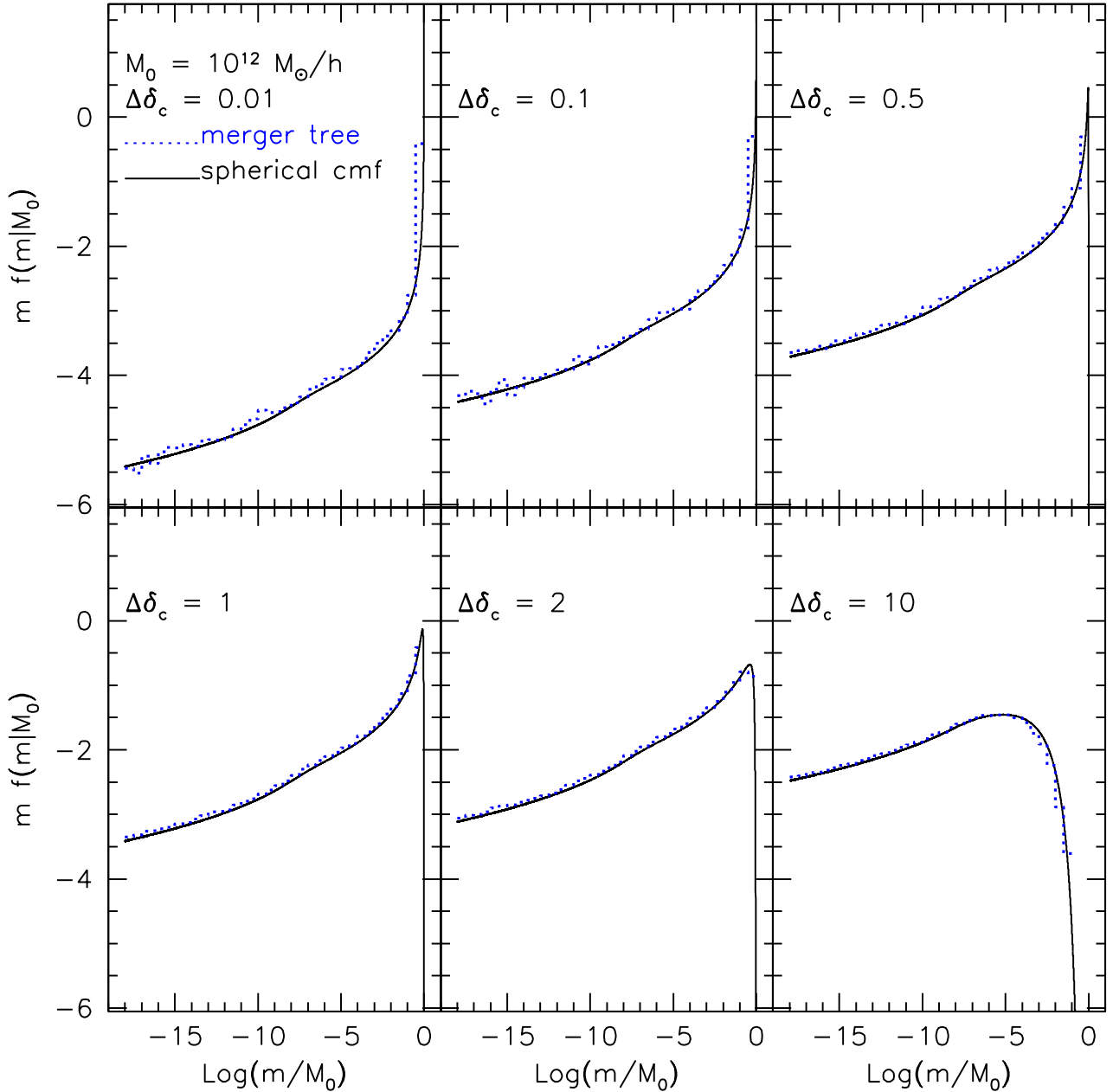


**Figure 1.** Spherical collapse conditional mass function at six different redshifts, obtained using the SL99 tree. We considered a  $\Lambda$ CDM power spectrum extrapolated down to  $10^{-6} M_{\odot}$  as in Giocoli et al. (2008b). In each panel the histogram shows the average of  $10^4$  realizations of partitioning an  $M_0$ -halo. The solid line represents the prediction of the spherical collapse model at the considered redshift. The partition was performed both with a single and a multi-step: the distributions are equivalent.

Taking  $\nu = \delta_c / \sqrt{S}$ , this equation describes, at a fixed redshift (and so at a given  $\delta_c$ ), the number of collapsed systems with mass variance between  $S$  and  $S + dS$ . The factor 2 takes into account the so-called *cloud-in-cloud problem*, which is the possibility that at a given instant some object, which is nonlinear on scale  $M$ , can be later contained within another object, on a larger mass scale. Eq. (8) describes also the conditional mass function at time  $\delta_{c,1}$ , considering a halo at time  $\delta_{c,0}$  with mass variance  $S_0$ , when  $\nu = (\delta_{c,1} - \delta_{c,0}) / \sqrt{s - S_0}$ .

Before taking into account a  $\Lambda$ CDM power spectrum,

let us consider the simpler case of a white-noise power spectrum. We recall that when  $P(k) \sim k^n$ , Eq (7) becomes  $M \sim S^{-(n+3)/3}$ , that for  $n = 0$  gives  $M \sim 1/S$ . Let us suppose we want to split an  $M_0$ -halo, at time  $\delta_{c,0}$ , in progenitor haloes at  $\delta_{c,1}$ . To generate the first progenitor we draw a random number  $\tilde{\nu}_1$  from the Gaussian distribution, Eq (8), and compute its associated mass variance,  $\tilde{s}_1$  con-



sidering that

$$\tilde{\nu}_1 = \frac{\delta_{c,1} - \delta_{c,m_\epsilon}}{\sqrt{s_1 - s_{m_\epsilon}}}, \quad (9)$$

where for this first progenitor  $m_\epsilon = M_0$  ( $s_{m_\epsilon} \sim 1/m_\epsilon$ ) and  $\delta_{c,m_\epsilon} = \delta_{c,0}$ . Its physical mass,  $\tilde{m}_1$ , can be directly computed as the inverse of its mass variance. Since for a white-noise power spectrum disconnected volumes are mutually independent, the overdensity of the remaining mass  $m_\epsilon = M_0 - \tilde{m}_1$  will be given by the volume conservation relation in the continuous limit:

$$\delta_{c,m_\epsilon} = \delta_{c,1} - \frac{(\delta_{c,1} - \delta_{c,0})}{m_\epsilon/M_0}. \quad (10)$$

To generate the second halo we draw another number from the Gaussian distribution, compute the mass variance from the Eq. (9), and hence derive the corresponding mass. The remaining mass will now be  $m_\epsilon = M_0 - \tilde{m}_1 - \tilde{m}_2$ , with the corresponding overdensity given always by Eq. (10). Keep going with this procedure it is possible to generate a sample of progenitor haloes until the desired  $m_\epsilon$  mass resolution.

## 2.2 $\Lambda$ CDM Power Spectrum

In the case of a general power spectrum the algorithm should be modified. The assumption that disconnected volumes are mutually independent does not hold anymore when the initial conditions differ from white-noise. Despite this, Sheth & Lemson (1999) noticed that, when expressed as a function of the variance rather than of the mass, all excursion set quantities are independent of the power spectrum. In this framework, each chosen mass  $\tilde{m}$ , can be treated not as a progenitor having a mass  $\tilde{m}$ , but as a region of volume  $\tilde{v}$  containing a mass  $\tilde{m}$ , populated by  $\zeta$  objects having all the same mass  $\mu$ , with  $\zeta = \tilde{m}/\mu$ .

The number of objects is obtained by requiring that they have the same mass variance, that is  $s(\mu) = 1/\tilde{m}$ . For a scale-free power spectrum  $P \sim k^n$  ( $\alpha = n + 3/3$ )  $\zeta = m^{(\alpha-1)/\alpha}$ , and for  $n = 0$  we have  $\zeta = 1$ , the region  $\tilde{v}$  contains exactly one halo, as seen in the previous section. For  $n \neq 0$  and general power spectrum,  $\zeta$  is neither unity nor even integer. However, we will show in the next section that considering  $\zeta = \text{NINT}(\tilde{m}/\mu)$  (i.e. considering the nearest integer to the mass ratio) the progenitor mass functions are in excellent agreement with the theoretical prediction at all redshifts and down to  $m_\epsilon = m_J = 10^{-6} M_\odot$ .

We recall that the  $\Lambda$ CDM and the white-noise power spectrum should satisfy the relation:

$$s_{\text{wn}}(M_0) = s_{\Lambda\text{CDM}}(M_0), \quad (11)$$

where  $M_0$  is the initial mass to be split. This guarantees that for the considered initial mass there is one halo in the volume  $V_0$  for both power spectra.

## 3 PARTITION OF A MILKY-WAY SIZE HALO WITH MICRO-SOLAR MASS RESOLUTION

Let us now take into account the case of a  $\Lambda$ CDM power spectrum. The density parameter and mass variance ( $\Omega_\Lambda = 0.7$ ,  $\Omega_m = 0.3$  and  $\sigma_8 = 0.772$ ) have been chosen to agree with the recent 3-year WMAP data release (Spergel et al.

2007). We have linearly extrapolated the mass variance down to the  $m_J = 10^{-6} M_\odot$  integrating the power spectrum using a top-hat filter in the real space (Giocoli et al. 2008b). In order to have one physical mass both for the  $\Lambda$ CDM and white-noise power spectrum, we should consider a white-noise power spectrum normalized such that Eq. (11) holds. For this reason, because we think in term of the mass variance than the fisical mass, the mass resolution  $m_\epsilon$ , for a  $\Lambda$ CDM power spectrum, corresponds to the mass resolution  $m_{\epsilon,\text{wn}}$  for the white-noise one, such that  $s_{\text{wn}}(m_{\epsilon,\text{wn}}) = s(m_\epsilon)$ , with  $m_{\epsilon,\text{wn}} > m_\epsilon$ .

### 3.1 The main branch and the satellite mass function

Let us consider a present-day Milky-Way sized halo ( $M_0 = 10^{12} M_\odot/h$ ) and suppose we wish to generate a sample of progenitors at different redshifts down to  $m_\epsilon \equiv m_J = 10^{-6} M_\odot$ , using a  $\Lambda$ CDM power spectrum. Such mass resolution corresponds to  $m_{\epsilon,\text{wn}} = 2.15 \times 10^{10} M_\odot/h$ . We proceed as described in the previous section and obtain the conditional mass function plotted in Fig. 1. The number of progenitor haloes in the  $\Lambda$ CDM power spectrum, for a given value of the mass variance, was obtained by computing the nearest integer of the ratio  $\tilde{m}/\mu$ , where  $s_{\text{wn}}(\tilde{m}) = s_{\Lambda\text{CDM}}(\mu)$ . In each panel the dotted histogram shows the result of averaging  $10^4$  realizations, and the solid line shows the theoretical prediction from the spherical collapse model. At each redshift we generated progenitors both with a single and a multi-steps technique starting from  $z = 0$ . Since the SL99 method is independent on the time-step, the results from the two different ways of progress are in perfect agreement.

In order to generate the merging history tree along the halo main branch, we ran a sample of  $10^4$  white-noise tree realizations for an  $M_0 = 10^{12} M_\odot/h$  initial halo and a mass resolution of  $0.0215 \times M_0$ . As stressed by SL99 (and demonstrated in Fig.1), this method is time-step independent: to obtain a fine enough description of the merging of satellite haloes we chose a time resolution  $\Delta\delta_c = 0.01$ . We followed the main branch (the most massive halo among the progenitors) along consecutive time-steps, storing all the information about the accreted progenitor haloes (termed “satellites”, as in Giocoli et al. (2008a)), until the mass of the main branch becomes as small as the mass resolution. We call merging redshift  $z_m$  the most recent redshift before a satellite is incorporated in the main halo.

Finally, the poissonian trees is converted in the  $\Lambda$ CDM one as explained in the previous section. We recall that each progenitor halo in the first tree is converted into  $\zeta$  haloes in the second, in order to conserve the mass variance in both power spectra.

### 3.2 Unevolved subhalo population

Giocoli et al. (2008b) studied the substructure population of a present-day Milky-Way halo considering its progenitor mass functions at any redshift  $z > 0$ , and assuming that all progenitor haloes survived and retained their original virial mass until redshift zero. This analytical distribution for the progenitor mass function was extrapolated down to microsolar mass resolution in order to study the  $\gamma$ -ray emission from

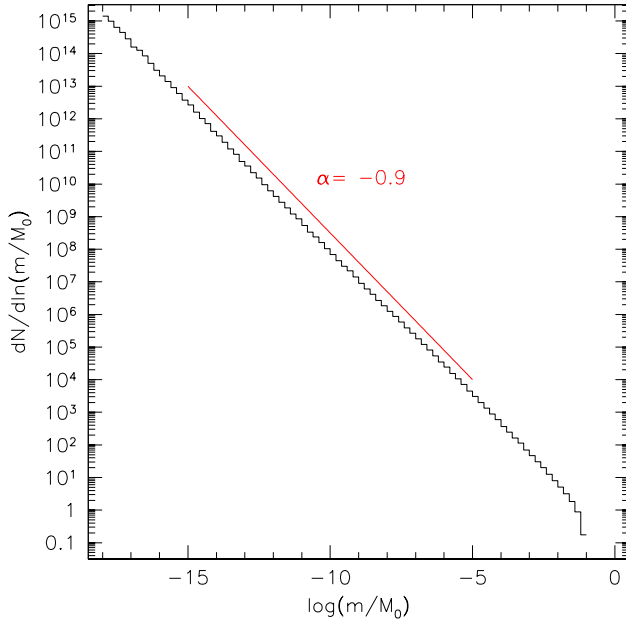


**Figure 2.** Satellite mass function for a present-day Milky-Way size halo. The histogram shows the result of  $10^4$  realizations of the merger history tree. The mass of each satellite is rescaled in units of the final host halo mass. The solid line shows the slope of the least squares fit to the histogram down to  $10^{-5}M_0$ .

all substructures that populate the galactic halo. Integrating the conditional mass function at any redshift in different mass bins, the full hierarchy of substructures was automatically taken into account: subhaloes within subhaloes within subhaloes, and so on. The  $\gamma$ -ray emission process due to dark matter annihilation is proportional to the square of the DM density, and the possibility that subhaloes might boost the expected flux was taken into consideration (see Giocoli et al. (2008b); Pieri et al. (2008a) and references therein).

In the present work we compute the  $\gamma$ -ray emission by considering as substructure only the progenitor haloes accreted by the main branch of our merger tree. **This procedure does not take directly into account the whole substructure population but only the first hierarchy of the population. Progressing in this way,** we can isolate the contribution to the boost from the single DM structure, including its own sub-substructures **subsequently, following its merging history tree.** Moreover, in this way we can model correctly the spatial satellite distribution inside the Galaxy, since many small mass halos will be in fact embedded inside larger ones.

In Fig. 2 we plot the satellite mass function, i.e. the mass function of progenitor haloes accreted directly by the main halo progenitor at any redshift. Satellite masses are expressed in units of the present-day mass of the host halo (van den Bosch et al. 2005; Giocoli et al. 2008a). This figure shows that the mass distribution is well described by a single power law  $dN/d\ln(m) \propto m^{-\alpha}$ , with slope  $\alpha = -0.9$ , plus an exponential cut off at large masses. The slope was obtained computing the least squares fit to the data down to  $m = 10^{-5}M_0$ . This slope is slightly steeper than that obtained by Giocoli et al. (2008a) using numerical  $N$ -Body simulations ( $\alpha_{\text{sim}} \approx -0.8$ ). Such a discrepancy is proba-

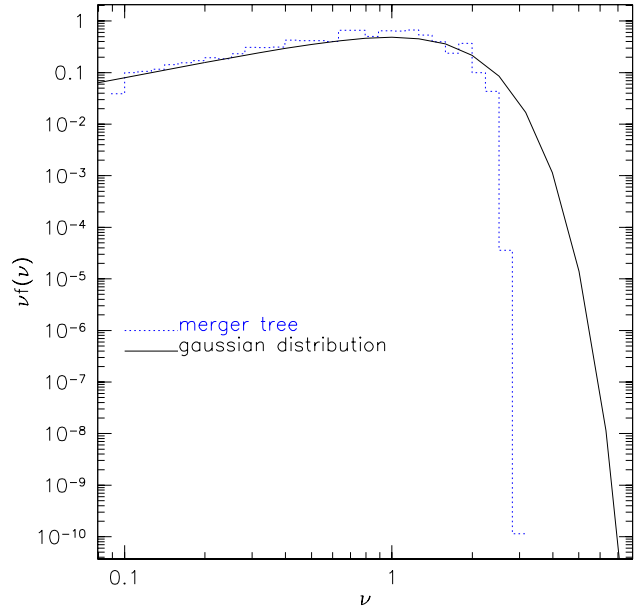


**Figure 3.** Satellite mass function in term of the rescaled parameter  $\nu(z_m, m) = \delta_c(z_m)/\sqrt{s(m)}$ . The dotted histogram show  $10^4$  realizations of the merger tree, while the solid curve is the Eq. (8).

bly due to the fact that the present merger tree is based on the spherical collapse model, while numerical simulations are better described using ellipsoidal collapse Sheth et al. (2001); Sheth & Tormen (2002); Giocoli et al. (2007).

The satellite mass function in Fig. 2 was obtained using the Monte Carlo code described in Sec. 2. We considered a halo of mass  $M_0$  at redshift  $z = 0$  and followed the main branch of its merging history tree back in time; we then: (i) generated a sample of progenitors at redshift  $\delta_{c,1} = \delta_{c,0} + \Delta\delta_c$ ; (ii) identified the main (most massive) progenitor halo; (iii) re-run the partition code computing its progenitors at redshift  $\delta_{c,2} = \delta_{c,1} + \Delta\delta_c$ . We iterated these steps until the mass of the main progenitor halo dropped below the mass resolution  $m_e$ . This produced the first merging history tree. We repeated the whole procedure, starting from the same mass  $M_0$ , to generate  $10^4$  histories, to be averaged on.

After computing the satellite mass function (also called *unevolved* subhalo mass function) we associated to each halo a concentration parameter related to the quantity  $\nu(z_m, m) = \delta_c(z_m)/\sqrt{s(m)}$ , where  $z_m$  is the satellite merging redshift onto the host halo, and  $m$  its virial mass at  $z_m$ .

By definition,  $\nu$  defines the rareness of the density peak the halo belonged to at the epoch of merging. Higher peaks of density fluctuations correspond to a collapse happened at higher redshifts. Such a rare halo will therefore be more concentrated than the bulk of halos with the same mass which formed at later epochs.

Diemand et al. (2005b) used  $N$ -Body simulations to show that the present-day subhalo distribution preserves memory of their initial conditions. In detail, high density peaks are found to be more centrally concentrated and to move on more eccentric orbits than the overall mass distribution. This correlation has been interpreted and parametrized by Diemand et al. (2005b) using the variable  $\nu = \delta_c(z)/\sqrt{s}$ . This variable (i) is related to the subhalo concentration -

which in turn determines the  $\gamma$ -ray emission, and (ii) enables one to compute the spatial distribution in the host halo (see Eq. (1) of Diemand et al. (2005b)). The details of the models are given in Sec. 5.2

In Fig.3 we plot the satellite mass function in terms of the universal variable  $\nu$ . The dotted histogram shows the result of  $10^4$  Monte Carlo realizations of the partition algorithm (as in Fig.2), while the solid curve is the Gaussian distribution, Eq. (8).

The figure shows that the satellite mass function is well described by a gaussian distribution for small and intermediate masses, with a cutoff at  $\nu=2$ . This fact can be qualitatively understood by recalling that the progenitor mass function has a Gaussian distribution when expressed in the rescaled variable  $\nu$ . For each evolutionary step  $dz$ , the satellite mass function is obtained by removing from all progenitors the most massive one. Integrating over redshift, the total satellite mass function is effectively an integral over different gaussians deprived of their most massive progenitor.

## 4 DRACO

The algorithm described in the previous sections can also be used to study and constrain some properties of the dark matter halos hosting the Milk-Way satellite galaxies. As an example let us consider Draco, a dwarf spheroidal galaxy with an old stellar population, dark matter dominated: Draco's mass to light ratio is estimated to be  $m/L \sim 100M_\odot/L_\odot$  (Pryor 1992; Irwin & Hatzidimitriou 1995). This makes it a very interesting target to investigate the existence of dark matter; specifically, we study the possibility of an observation of  $\gamma$ -ray due to DM annihilation inside Draco using the Fermi Large Area Telescope (Fermi-LAT, formerly known as GLAST). To this extent, we model the distribution of dark matter subclumps inside Draco.

### 4.1 Mass and Merging Time Estimates

Hierarchical models of galaxy formation predict that galaxies are hosted by dark matter haloes. Such haloes grow along cosmic time through repeated merging events. In this scenario satellite galaxies reside in subhaloes accreted by the main halo progenitor. Satellite haloes grow themselves hierarchically, accreting mass and sub-progenitors up to the time when they merge onto the host halo. After they fall in the gravitational potential well of the host, they start to loose mass due to gravitational heating, tidal stripping and close encounters with other subhaloes, so that only a fraction of their initial virial mass is still self-bound at redshift zero (van den Bosch et al. 2005; Diemand et al. 2007b, 2008; Giocoli et al. 2008a).

In order to build the history tree for a subhalo hosting a satellite galaxy, we need to know its virial mass at merging time  $z_m$  and use it as our starting point. From its merging redshift we then can go backwards in time and reconstruct its subhalo population, in order to model its present-day sub-subhalo mass function and distribution.

Using deep wide-field multicolor CCD photometry from the Sloan Digital Sky Survey, assuming a King (1966) spherical model of equivalent size as a reference and

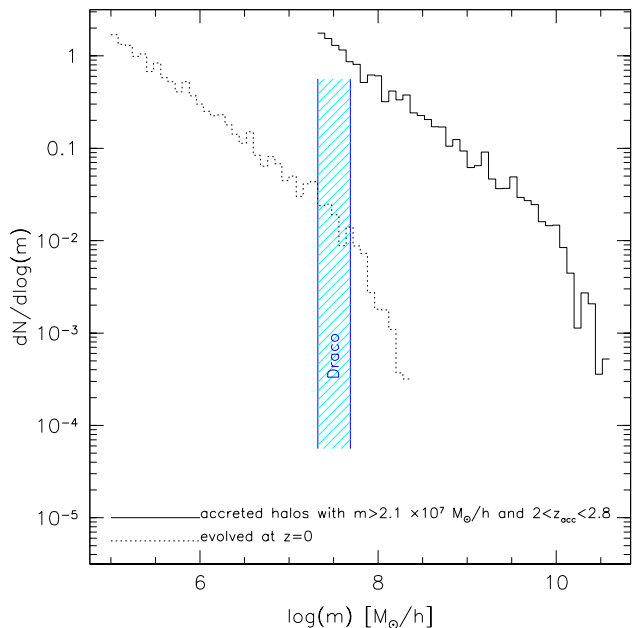


**Figure 4.** *Unevolved and evolved subhalo mass function of Draco candidates accreted by a Milky-Way halo. The solid histogram shows the satellite distribution, the dotted one refers to the present day mass function evolved by using the average mass loss rate derived by Giocoli et al. (2008a). The hatched region bounds the most likely values for the present-day mass of Draco (Odenkirchen et al. 2001; Lokas et al. 2005).*

adopting a line-of-sight velocity dispersion of 10.7 km/s Armandroff et al. (1995) finds  $3.5 \pm 0.7 \times 10^7 M_\odot$  within 28 arcmin while Odenkirchen et al. (2001), considering 8.5 km/2, finds  $2.2 \pm 0.5 \times 10^7 M_\odot$  within 40 arcmin. Differences in the experimental mass modeling determine the mass range we allow for the Draco-like satellite in our analysis. Considering all the stars within the tidal radius, Odenkirchen et al. (2001) determined the total luminosity of the Draco dwarf galaxy to be  $(L/L_\odot)_i = 2.4 \pm 0.5 \times 10^5$ . Lokas et al. (2005) also studied the distribution of dark matter in Draco by modeling the moments of the line-of-sight velocity distribution of its stars from the velocity dispersion data of Wilkinson et al. (2004), and obtained a best-fitting total mass equal to  $7 \times 10^7 M_\odot$ . The inferred mass-to-light ratio (in the V-band) was  $300 M_\odot/L_\odot$ , almost constant with radius. On the other hand, we lack a direct estimate for the merging redshift of Draco onto the Milky Way. From its initial position and velocity, the accretion time of Draco can be derived indirectly by considering the one-to-one relation between virial radius and accretion time implied by the spherical secondary infall model (Bertschinger 1985). Hayashi et al. (2003) showed that an upper limit for Draco merging redshift is  $z_m \lesssim 2.8$ .

We have computed the Draco virial mass from the previous mass and redshift estimates in the following way. From each one of the  $10^4$  Monte Carlo merging trees of a Milky-Way sized halo ( $M_0 = 10^{12} M_\odot/h$ ) we noted down all satellites with mass larger than  $3 \times 10^7 M_\odot$  accreted by the main branch between  $z = 2$  and  $z = 2.8$ , totaling 8932 Draco candidates. The redshift interval roughly corresponds to a time interval of 1Gyr from the upper limit of the accretion time

computed by Hayashi et al. (2003). The lower limit on the Draco mass guarantees that evolved masses will lie today within the experimentally estimated mass range. In Fig. 4 the solid histogram shows the mass function of these selected satellite haloes. Once inside its host, each satellite will lose mass due to gravitational heating and tidal stripping effects. We modeled these effects using the results in Eq. (10) of Giocoli et al. (2008a). In that paper the authors measured the subhalo mass loss rate in a sample of high resolution  $N$ -body haloes ranging from  $10^{11.5}$  to  $10^{15} M_{\odot}/h$ . Following their recipe, the ratio of  $z = 0$  self bound mass to the original virial mass of the subhalo is uniquely determined by the amount of time the subhalo has spent inside its host. The dotted histogram in Fig. 4 shows the evolved subhalo Draco-candidates mass function. Considering that the measured fractional mass loss rate by Giocoli et al. (2008a) is independent of the subhalo mass, the evolved mass function has the same slope of the unevolved one.

#### 4.2 The Sub-Tree

In order to compute the Draco satellite mass function, each candidate of our sample has been further evolved back in time along its main branch using the partition code (as it was done for the Milky-Way halo) considering the same mass and time step resolution. In this case each merger history tree starts at the corresponding satellite merging time. To increase the statistical significance of our result we run three realizations for each of the 8932 Draco-like satellites, totaling 26796 Monte Carlo merger tree realizations. In Fig. 5 we show the *unevolved* sub-subhalo mass function accreted by the Draco sample. Comparing Fig. 5 and Fig. 2, we see that the two accreted mass functions are indistinguishable: in fact, as found by Giocoli et al. (2008a); van den Bosch et al. (2005), the accreted mass function is universal, independent both of final mass and observation redshift. The slope of the power law is again  $\alpha = -0.9$ .

### 5 $\gamma$ -RAY FLUX FROM DARK MATTER ANNIHILATION IN SUB(SUB)STRUCTURES

The photon flux expected from DM annihilation in the population of galactic subhaloes can be modeled as

$$\frac{d\Phi_{\gamma}}{dE_{\gamma}}(E_{\gamma}, \psi, \Delta\Omega) = \frac{d\Phi^{\text{PP}}}{dE_{\gamma}}(E_{\gamma}) \times \Phi^{\text{cosmo}}(\psi, \Delta\Omega) \quad (12)$$

where  $\psi$  defines the direction of observation with respect to the galaxy center, and  $\Delta\Omega$  is the detector angular resolution.

The particle physics dependence in Eq. 12 is given by the annihilation spectrum and DM properties and is embedded in the term:

$$\frac{d\Phi^{\text{PP}}}{dE_{\gamma}}(E_{\gamma}) = \frac{1}{4\pi} \frac{\sigma_{\text{ann}} v}{2m_{\chi}^2} \cdot \sum_f \frac{dN_{\gamma}^f}{dE_{\gamma}} B_f, \quad (13)$$

where  $m_{\chi}$  is the DM particle mass,  $\sigma_{\text{ann}} v$  the self-annihilation cross-section times the relative velocity of the two annihilating particles, and  $dN_{\gamma}^f/dE_{\gamma}$  the differential photon spectrum for a given final state  $f$  with branching ratio  $B_f$  which we model after the results of (Fornengo et al. 2004).

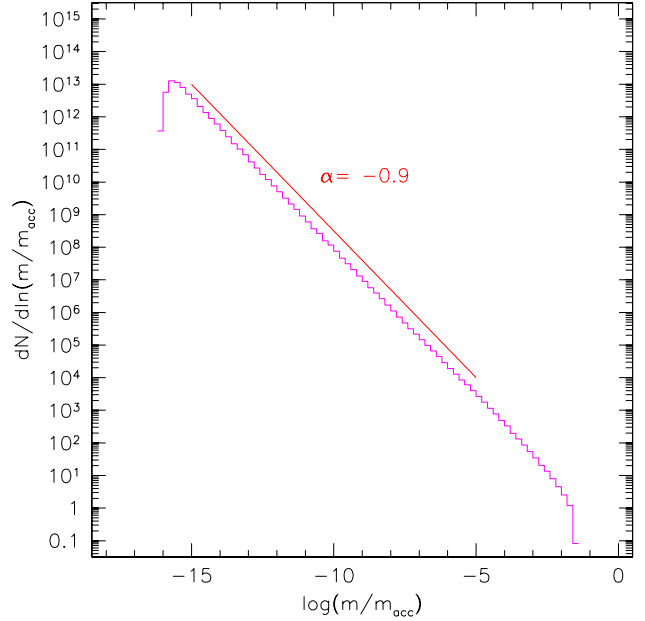


**Figure 5.** Satellite mass function accreted by the main branch of the Draco-candidate trees, until the merging on the Milky-Way main progenitor halo. The total number of realizations is 26796. Comparing the histogram with Fig. 2 we notice that the slopes of the distributions are identical. This is in agreement with what found by Giocoli et al. (2008a); van den Bosch et al. (2005) that is the *unevolved* subhalo mass function is independent both of final host halo mass and redshift.

In this paper we will set  $\Phi^{\text{PP}} = 1$  and refer to  $\Phi^{\text{cosmo}}$  as a scaled photon flux. In the following subsections we review different ways to compute  $\Phi^{\text{cosmo}}$  in the presence of substructures. We will then show the computation relative to the merger tree technique presented in the previous sections and will show the comparison between the different predictions.

#### 5.1 Results on the $\gamma$ -ray flux from the analytical description of the subhalo population

Pieri et al. (2008a) have considered the existence of a population of substructures inside a DM halo, described by the mass function

$$dN/d\ln(m) \propto m^{-1}, \quad (14)$$

and assumed that Eq. 14 describes the mass function of all substructures in our Galaxy as well as that of sub-substructures, at  $z=0$ . In this case all the halos that ever accreted onto the main one and survived are considered, including the higher level ones (substructures within substructures). Using this prescription it is then impossible to discriminate a sub-halo from a sub-sub-halo, affecting in a wrong way the spatial distribution of substructures inside the main halo.

Pieri et al. (2008a) assumed that the substructure spatial distribution traces that of the underlying host mass from  $r_{\text{vir}}$  and down to a minimum radius,  $r_{\text{min}}(m)$ , within which disruption by Galaxy tides and stellar encounters becomes relevant.



Folding these indications together they modeled the number density of subhaloes per unit mass at a distance  $R$  from the Galactic Center (GC) as:

$$\rho_{sh}(m, R) = Am^{-2} \frac{\theta(R - r_{min}(m))}{(R/r_s^{PH})(1 + R/r_s^{PH})^2} M_\odot^{-1} \text{ kpc}^{-3}, \quad (15)$$

where  $r_s^{PH}$  represents the scale radius of the parent halo (PH) referred to a Navarro, Frenk and White (NFW) (Navarro et al. 1997) profile. The effect of tidal disruption is accounted for by the Heaviside step function  $\theta(r - r_{min}(m))$ .

To determine the tidal radius,  $r_{min}(m)$ , they used the Roche criterion and compute it as the minimum distance at which the subhalo self-gravity at  $r_s$  equals the gravity pull of the host halo computed at the orbital radius of the subhalo.

To normalize Eq. 20, they imposed that 10% of the PH mass is distributed in subhaloes with masses in the range  $[10^{-5} - 10^{-2}] M_{PH}$ .

Following the previous prescriptions, they found about 53% of the MW mass ( $M_{PH} = 10^{12} M_\odot/h$ ,  $r_s = 21.7 \text{ kpc}$ ,  $c_{200} = 9.8$ ) condensed within  $\sim 1.5 \times 10^{16}$  subhaloes with masses in the range  $[h 10^{-6}, 10^{10}] M_\odot/h$ .

Pieri et al. (2008b) repeated the calculation for the Draco Galaxy, for which  $\sim 40\%$  of the halo mass ( $M_{Draco} = 7 \times 10^7 M_\odot$ ,  $r_s = 0.4 \text{ kpc}$ ,  $c_{200} = 21.2$ ) condensed into  $\sim 10^{12}$  halos with masses between  $[h 10^{-6}, 10^6] M_\odot/h$ .

For each substructure, they used a NFW density profile whose concentration parameter  $c_{200}$  (referred to the radius enclosing a density equal to 200 times the critical density) is given by the Bullock et al. (2001) prescriptions for the subhaloes at redshift zero (assuming the subhaloes are slightly more concentrated than the field halos). The Bullock et al. (2001) model holds down to masses of the order of  $10^5 M_\odot$ . In order to cover the whole subhalo mass range, they performed a double mass slope extrapolation down to the smallest masses, obtaining a concentration parameter of about 70 for a  $10^{-6} M_\odot$  halo at redshift zero. This value is in agreement with the extrapolation at redshift zero of what found in the numerical simulations by Diemand et al. (2005a), who isolated  $10^{-6} M_\odot$  halos at  $z=26$ .

Such a model for the concentration parameter has been called  $B_{z_0, ref}$  model.

The contribution of unresolved substructures to the annihilation signal along a cone of sight is given by

$$\begin{aligned} \Phi^{\text{cosmo}}(\psi, \Delta\Omega) &= \int_M dm \int_c dc \int_{\Delta\Omega} d\theta d\phi \int_{1.o.s} d\lambda \\ &[\rho_{sh}(m, R(R_\odot, \lambda, \psi, \theta, \phi)) \times P(c) \times \\ &\times \Phi_{halo}^{\text{cosmo}}(m, c, r(\lambda, \lambda', \psi, \theta', \phi')) \times J(x, y, z|\lambda, \theta, \phi)] \quad (16) \end{aligned}$$

where  $\Delta\Omega$  is the solid angle of observation pointing in the direction of observation  $\psi$  and defined by the detector angular resolution  $\theta$ ;  $J(x, y, z|\lambda, \theta, \phi)$  the Jacobian determinant;  $R$  the galactocentric distance, which, inside the cone, can be written as a function of the line of sight ( $\lambda$ ), the solid angle ( $\theta$  and  $\phi$ ) and the pointing angle  $\psi$  through the relation  $R = \sqrt{\lambda^2 + R_\odot^2 - 2\lambda R_\odot C}$ , where  $R_\odot$  refers to the distance of the Sun from the Galactic Center and  $C = \cos(\theta) \cos(\psi) - \cos(\phi) \sin(\theta) \sin(\psi)$ ;  $r$  is the radial coordinate inside the single subhalo located at distance  $\lambda$  from the observer along the line of sight defined by  $\psi$  and con-

tributing to the diffuse emission. Finally,  $P(c)$  is the lognormal distribution of the values for the concentration parameters. The expression

$$\begin{aligned} \Phi_{halo}^{\text{cosmo}}(m, c, r) &= \int \int_{\Delta\Omega} d\phi' d\theta' \int_{1.o.s} d\lambda' \\ &\left[ \frac{\rho_\chi^2(m, c, r(\lambda, \lambda', \psi, \theta', \phi'))}{\lambda^2} J(x, y, z|\lambda', \theta', \phi') \right]; \quad (17) \end{aligned}$$

describes the emission from each subhalo and  $\rho_\chi(m, c, r)$  is the Dark Matter density profile inside the halo.

Numerical integration of Eq. 16 gives the contribution to  $\Phi^{\text{cosmo}}$  from unresolved clumps in a  $10^{-5} \text{ sr}$  solid angle along the direction  $\psi$ .

We show the results obtained in this theoretical framework with a dashed line in Fig. 6 (Pieri et al. 2008a) for the MW and in Fig. 7 (Pieri et al. 2008b) for the Draco galaxy.

## 5.2 Results on the $\gamma$ -ray flux from the analytical method including the effect of the merging epoch

A further degree of detail was given by Giocoli et al. (2008b), who computed Eq. 16 including the dependence of the subhalo spatial distribution from the initial conditions when the haloes accreted into the present-day Milky Way halo. Such a model is characterized by the universal variable  $\nu(m)$ . According to Diemand et al. (2005b) the DM density profile of our Galaxy can be written as

$$\rho_\chi(r) = \frac{\rho_s}{\left(\frac{r}{r_s}\right)^\gamma \left[1 + \left(\frac{r}{r_s}\right)^\alpha\right]^{(\beta-\gamma)/\alpha}} \quad (18)$$

with  $(\gamma, \beta, \alpha) = (1.2, 3, 1)$ . Subsequently, the following parameterization is used to reflect the fact that material accreted in areas with high density fluctuations is more concentrated toward the centre of the galaxy, and has a steeper outer slope:

$$r_s \longrightarrow r_\nu = f_\nu r_s$$

$$f_\nu = \exp(\nu/2)$$

$$\beta \longrightarrow \beta_\nu = 3 + 0.26\nu^{1.6} \quad (19)$$

Including a step function to take into account tidal disruption, as in Eq. 20, the number density of subhaloes per unit mass at a distance  $r$  from the GC, for a given  $\nu(m)$ , becomes:

$$\rho_{sh}(m, r, \nu) = \frac{Am^{-2}\theta(r - r_{min}(m))}{\left(\frac{r}{r_\nu(m)}\right)^\gamma \left[1 + \left(\frac{r}{r_\nu(m)}\right)^\alpha\right]^{(\beta_\nu-\gamma)/\alpha}}, \quad (20)$$

in units of  $M_\odot^{-1} \text{ kpc}^{-3}$ . The mass dependence in  $r_\nu$  reflects the mass dependence of the virial parameter  $r_s = r_{vir}/c_{vir}$ .

Giocoli et al. (2008b) normalized the number of subhaloes such that 10% of the MW mass is distributed in subhaloes with masses in the range  $[10^{-5} - 10^{-2}] M_{MW}$ , ending up with  $2.4 \times 10^{16}$  subhaloes with masses between  $10^{-6} M_\odot$  and  $10^{10} M_\odot/h$ , accounting for 74 % of the MW mass ( $M_{MW} = 1.4 \times 10^{12} M_\odot$ ,  $r_s = 26 \text{ kpc}$ ).

The contribution to  $\Phi^{\text{cosmo}}$  is given by:

$$\Phi^{\text{cosmo}}(\psi, \Delta\Omega) = \int_M dm \int_\nu d\nu \int_{\Delta\Omega} d\theta d\phi \int_{1.o.s} d\lambda \int_c dc$$

$$[\rho_{sh}(m, R(R_\odot, \lambda, \psi, \theta, \phi), \nu) \times P(\nu(m)) \times P(c(m)) \times \Phi_{halo}^{cosmo}(m, r(\lambda, \lambda', \psi, \theta', \phi'), \nu, c) \times J(x, y, z|\lambda, \theta, \phi)] \quad (21)$$

which accounts for the influence of cosmology in the flux computation.  $P(\nu(m))$  is the probability distribution function for the peak rarity  $\nu(m)$ , calculated using the extended Press-Schechter formalism.  $P(c(m))$  is the lognormal probability distribution for  $c$  centered on  $c_{vir}(m)$ . While  $P(\nu(m))$  is determined by the merging history of each subhalo,  $P(c(m))$  describes the scatter in concentration for haloes of equal mass (Bullock et al. 2001) and the two probabilities may be assumed to be independent. As in the previous analytical estimate of the subhalo population, no distinction can be made with this method between sub-halos and sub-sub-halos.

The result of this calculation for the MW is shown with the long-dashed line in Fig. 6.

### 5.3 Results on the $\gamma$ -ray flux from merger tree technique

In this work we have described a merger tree approach to infer the subhalo population of both the MW and Draco. In this case, we don't need to use the  $P(\nu)$  and  $dN/dm$  factors, nor to apply any normalization. Indeed, the output of the merger tree gives us directly the number of objects with a given mass and a given  $\nu$ , which we call now  $N(\bar{m}, \bar{\nu})$ .

The total number of sub(-sub)structures found with this method is  $\sim 2.6 \times 10^{15}$  for the MW and  $2.7 \times 10^{13}$  in the case of Draco, at the merging epoch. In the case of the MW, and differently from the analytical methods described above, this number represents only the subhaloes, while sub-subhaloes must be treated separately, as it has been done for the Draco-like subhalo.

In order to compute the  $\gamma$ -ray flux we can re-write the subhalo distribution function as

$$\rho_{sh} = Ag(r, \nu(m))f(m)$$

so that

$$N_{tot} = \sum_{m_i} N(m_i) = \int_{gal} dV \int_M dm \int_\nu P(\nu(m)) \rho_{sh}$$

which can be rearranged into the following expression:

$$\sum_{m_i} N_{m_i} = \int_M dm A f(m_i) \int_\nu P(\nu(m_i)) \int_{gal} dV g(r, \nu(m_i)).$$

Let's define

$$G(m_i) = \int_{gal} dV g(r, \nu(m_i)).$$

The expression of  $\Phi_{cosmo}$  can be then written as:

$$\Phi^{cosmo}(\psi, \Delta\Omega) = \int_M dm \int_\nu d\nu \int_{\Delta\Omega} d\theta d\phi \int_{l.o.s} d\lambda \int_c dc [Ag(r, \nu(m))f(m)P(\nu(m))P(c(m))\Phi_{halo}^{cosmo} \frac{G(m)}{G(m)} J].$$

With respect to Eq. 21 we have only written  $\rho_{sh}$  in an explicit way and multiplied by  $\frac{G(m)}{G(m)} = 1$ . In this way we can

recognize and use our merger tree output  $\sum_{m_i} N_{m_i}$  in the following way ( $\int_{gal} dV = \int_{\Delta\Omega} d\theta d\phi \int_{l.o.s} d\lambda$ ):

$$\Phi^{cosmo}(\psi, \Delta\Omega) = \sum_{m_i} \int_{\Delta\Omega} d\theta d\phi \int_{l.o.s} d\lambda \int_c dc [N(m_i)g(r, \nu(M_i))P(c(M)) \frac{1}{G(m_i)} \Phi_{halo}^{cosmo} J.] \quad (22)$$

The result of this calculation is depicted with a dotted line in Fig.6. We note that the analytical methods predict more substructures, and therefore a higher signal, than the merger tree. This is mainly due to the different mass function slope (-2.0 versus -1.9).

In the case of the Draco galaxy, the merger tree was computed at the Draco merging epoch (no sub-subhaloes accrete after merging), when its mass was  $9.78 \times 10^9 M_\odot$ . Although the sub-subhaloes evolve in redshift and loose mass as the parent halo does, for each sub-subhalo we considered a NFW profile whose concentration parameter has been computed for the sub-subhalo mass at the merging epoch, motivated by the fact that the inner profile of the structures should not or poorly be affected by evolution.

From the observational point of view, we are interested in the Draco-like galaxy as it is today, e.g. with a mass content reduced by a factor  $\sim 10^{-2}$  due to tidal interactions after merging (Giocoli et al. 2008a).

To estimate the number of sub-subhaloes in Draco today we have retained all and only the subhaloes which, at the epoch of merging, were inside the radius containing the Draco mass today, that is within  $r_c = 2.84$  kpc.  $r_c$  is also similar to the tidal radius obtained using the prescription given by Springel et al. (2008) to obtain the number of sub-subhaloes today. The total number of subhaloes is  $6 \times 10^{-3}$  smaller than the initial one. This is the upper value for the number of subhaloes, since we are not considering here that half of the subhaloes exit the virial radius of the parent halo during their first orbit (Tormen et al. 2005). In the case of field parent halos they would then be re-attracted inside the halo, but if the parent halo is a subhalo itself (like Draco) they would then be dispersed in the main halo (that is the MW).

As for  $\rho_{sh}$ , we have used the scale quantities  $r_s$  and  $\rho_s$  computed for the evolved Draco-like galaxy, that is for a  $7 \times 10^7 M_\odot$  halo.

The result of the computation of  $\Phi_{cosmo}$  for Draco is shown with a dotted line in Fig.7. For comparison we also show the result from the analytical calculation and the same quantity relative to the smooth NFW halo of Draco. As in the case of the MW, we note that the merger tree approach gives a comparable yet smaller result than the analytical one.

Pieri et al. (2008a); Giocoli et al. (2008b); Pieri et al. (2008b) showed how the detectability of a  $\gamma$ -ray flux from such a population of sub-subhaloes with the Fermi-LAT telescope serendipitously depends on a very boosted particle physics contribution. The present and more accurate results give an even lower expected flux, thus furtherly reducing the hope for detection, unless an exotic boost from particle physics enters the play. In fact, Baltz et al. (2008) have computed the map of the Fermi-LAT sensitivity to point sources of DM annihilations, by using the released Fermi-

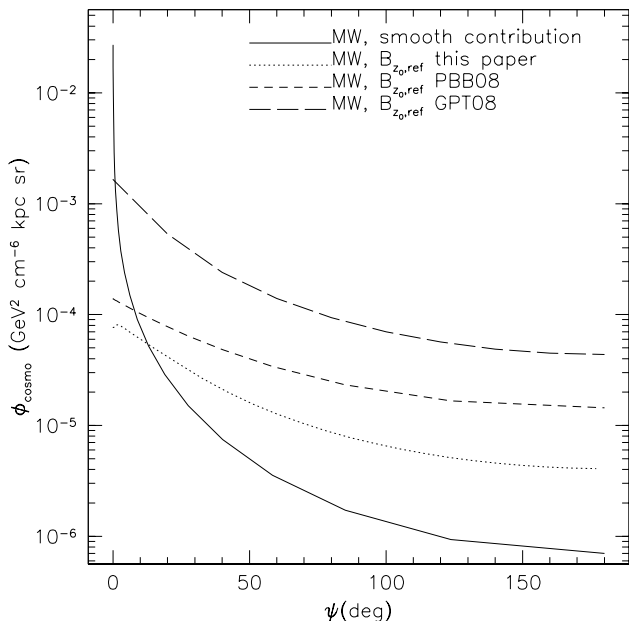


**Figure 6.**  $\Phi_{\text{cosmo}}$  as a function of the angle of view  $\psi$  from the galactic centre, computed for the MW.

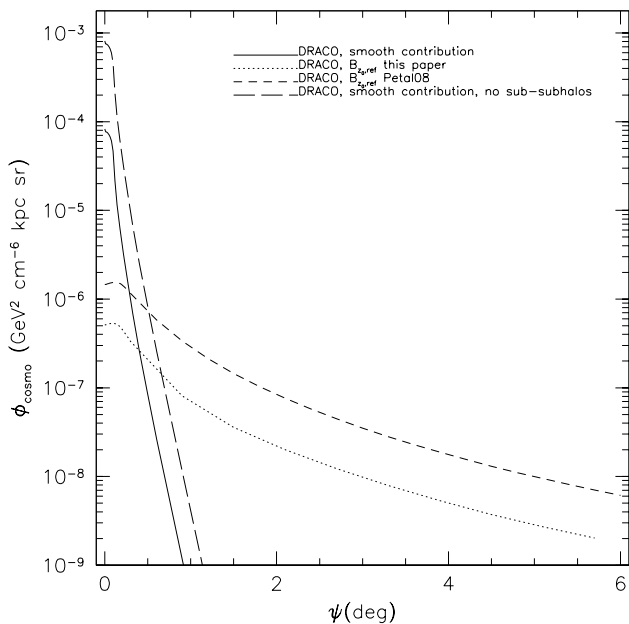


**Figure 7.**  $\Phi_{\text{cosmo}}$  as a function of the angle of view  $\psi$  from the galactic centre, computed for the Draco galaxy.

LAT response functions. Draco lies in a region of the sky where the  $5\sigma$  detection flux above 100 MeV in 1 year of data taking is  $\phi_{5\sigma}^{1\text{yr}} = 6 \times 10^{-9} \text{ ph cm}^{-2} \text{ s}^{-1}$ . In order to obtain the afore-mentioned flux we have to multiply the particle physics contribution by the highest value of  $\Phi_{\text{cosmo}}$  we have obtained, that is to say along the line of sight pointing towards the centre of Draco. Our result is that we would need a boost factor of 600 (120) when using the already optimistic scenarios where  $m_\chi = 100$  (40) GeV and  $\sigma v = 3 \times 10^{-26} \text{ cm}^3 \text{ s}^{-1}$ .

In the case of Draco and for the  $B_{z_0, \text{ref}}$  model, we can conclude that no higher order computations are necessary (sub-sub-subhaloes and so on). In fact, we have computed the boost factor due to substructures for any mass of the parent halo from  $10^{-3}$  to  $10^{10} M_\odot$ , that is to say the ratio of the integral of the density squared over the whole galaxy including subhaloes to the same quantity computed in the case of a smooth halo, which gives the boost to the  $\gamma$ -ray flux due to substructures for point-like halos. We found that its value is pretty flat and close to 1, only slightly larger for larger mass haloes, which however does not appear point-like at the distance of Draco. This means that no boost is obtained when considering sub-substructures for point-like subhaloes. As far as massive haloes (with mass greater than  $10^3 M_\odot$ ) are concerned, which are not point-like at the distance of Draco, we have to consider the fact that, as in the case of Draco, the boost must be distributed spatially. Indeed, this spatial distribution of the boost factor leads to an even smaller value of the expected flux along the line of sight toward the centre of the halo, where the flux is higher. This means that including sub-substructures does not increase the total  $\gamma$ -ray flux from the subhalo.

## 6 DISCUSSIONS AND CONCLUSIONS

In this paper we used the SL99 merger tree technique to study the mass accretion history in satellite of a Milky-Way sized halo. The partition code has been generalised for a  $\Lambda$ CDM power spectrum, considering a microsolar mass resolution of  $m_J = 10^{-6} M_\odot$ . The MW-main progenitor halo has been followed along consecutive time steps from the present day down to when its mass dropped below the resolution limit. From the satellite haloes we have identified a sample of Draco-like systems and also followed them along their merger tree, starting from their accretion redshift into the MW-main halo progenitor. Both the Milky-Way and the Draco satellite mass function turned to be equivalent, testing the universality of this distribution. The partition technique allowed us to build up models for the present-day subhalo mass function for both MW and Draco – considering only haloes that they accreted along the main branch.

We then computed the expected  $\gamma$ -ray flux from DM annihilation in such a population of substructures. We found that the prediction for the  $\gamma$ -ray flux is indeed more pessimistic than the ones obtained in previous estimates **which were not correctly taking into account the embedding of small scale sub-subhaloes within subhaloes, and therefore adding their contribution to the host halo total flux instead of to the subhalo they belong to.** Detection with the Fermi-LAT telescope is probably out of the discovery range of the satellite, unless some exotic particle physics could boost the signal significantly.

While we were writing this paper, the results of the Aquarius simulation came out (Springel et al. 2008), predicting a smaller number of subhaloes and a shallower internal slope for the subhaloes density profiles. We will not repeat our analysis in their model since it would fourthly reduce the expected flux, but the reader should be aware that the results presented in this paper, though pessimistic, are upper limits for the expected signal from DM annihilation in galactic subhaloes.

**ACKNOWLEDGEMENTS**

CG thanks the partial support for this work given by the Italian PRIN and ASI. Thanks also to R. K. Sheth for very useful discussions during the time spent in Philadelphia at the end of 2007.

**REFERENCES**

- Armandroff, T. E., Olszewski, E. W., & Pryor, C. 1995, *AJ*, 110, 2131
- Baltz, E. A., Berenji, B., Bertone, G., Bergström, L., Bloom, E., Bringmann, T., Chiang, J., Cohen-Tanugi, J., Conrad, J., Edmonds, Y., and 18 coauthors, 2008, *Journal of Cosmology and Astro-Particle Physics*, 7, 13
- Bertschinger, E. 1985, *ApJS*, 58, 39
- Bond, J. R., Cole, S., Efstathiou, G., & Kaiser, N. 1991, *ApJ*, 379, 440
- Borel, E., 1942, Sur l'emploi du theoreme de Bernoulli pour faciliter le calcul d'une infinite de coefficients. Application au probleme de l'attente a un guichet. *Comptes Rendus, Academie des Sciences, Paris, Series A*, 214, 452-456
- Bower, R. G. 1991, *MNRAS*, 248, 332
- Bullock, J. S., Kolatt, T. S., Sigad, Y., Somerville, R. S., Kravtsov, A. V., Klypin, A. A., Primack, J. R., & Dekel, A. 2001, *MNRAS*, 321, 559
- Bullock, J. S., Kravtsov, A. V., & Weinberg, D. H. 2000, *ApJ*, 539, 517
- Carroll, S. M., Press, W. H., & Turner, E. L. 1992, *ARA&A*, 30, 499
- Cole, S. 1991, *ApJ*, 367, 45
- Cole, S., & Kaiser, N. 1988, *MNRAS*, 233, 637
- Diemand, J., Moore, B. & Stadel, J., *Nature* **433** (2005) 389
- Diemand, J., Madau, P., & Moore, B. 2005, *MNRAS*, 364, 367
- Diemand, J., Kuhlen, M., & Madau, P. 2007, *ApJ*, 657, 262
- Diemand, J., Kuhlen, M., & Madau, P. 2007, *ApJ*, 667, 859
- Diemand, J., Kuhlen, M., & Madau, P. 2008, *ApJ*, 679, 1680
- Eke, V. R., Cole, S., & Frenk, C. S. 1996, *MNRAS*, 282, 263
- Epstein, R. I. 1983, *MNRAS*, 205, 207
- Fornengo N., Pieri L., Scopel S., 2004, *Phys. Rev. D*, 70, 103529
- Kauffmann, G., & White, S. D. M. 1993, *MNRAS*, 261, 921
- King, I. R. 1966, *AJ*, 71, 64
- Kravtsov, A. V., Berlind, A. A., Wechsler, R. H., Klypin, A. A., Gottlöber, S., Allgood, B., & Primack, J. R. 2004, *ApJ*, 609, 35
- Hayashi, E., Navarro, J. F., Taylor, J. E., Stadel, J., & Quinn, T. 2003, *ApJ*, 584, 541
- Irwin, M., & Hatzidimitriou, D. 1995, *MNRAS*, 277, 1354
- Lacey, C., & Cole, S. 1993, *MNRAS*, 262, 627
- Lacey, C., & Cole, S. 1994, *MNRAS*, 271, 676
- Lokas, E. L., Mamon, G. A., & Prada, F. 2005, *MNRAS*, 363, 918
- Gao, L., White, S. D. M., Jenkins, A., Stoehr, F., & Springel, V. 2004, *MNRAS*, 355, 819
- Giocoli, C., Moreno, J., Sheth, R. K., & Tormen, G. 2007, *MNRAS*, 376, 977
- Giocoli, C., Tormen, G., & van den Bosch, F. C. 2008, *MNRAS*, 386, 2135
- Giocoli, C., Pieri, L., & Tormen, G. 2008, *MNRAS*, 386, 630
- Green, A. M., Hofmann, S., & Schwarz, D. J. 2004, *MNRAS*, 353, L23
- Green, A. M., Hofmann, S., & Schwarz, D. J. 2005, *Journal of Cosmology and Astro-Particle Physics*, 8, 3
- Moore, B., Ghigna, S., Governato, F., Lake, G., Quinn, T., Stadel, J., & Tozzi, P. 1999, *ApJL*, 524, L19
- Moreno, J., Giocoli, C., & Sheth, R. K. 2007, *arXiv:0712.4100*
- Navarro, J. F., Frenk, C. S., & White, S. D. M. 1997, *ApJ*, 490, 493
- Neistein, E., & Dekel, A. 2008, *ArXiv e-prints*, 802, *arXiv:0802.0198*
- Odenkirchen, M., et al. 2001, *AJ*, 122, 2538
- Percival, W. J., & Miller, L. 1999, *MNRAS*, 309, 823
- Percival, W. J., Miller, L., & Peacock, J. A. 2000, *MNRAS*, 318, 273
- Pieri, L., Bertone, G., & Branchini, E. 2008, *MNRAS*, 384, 1627
- Pieri L., Pizzella A., Corsini E. M., Dalla Bontà E., Bertola F., *A&A* in press.
- Profumo, S., Sigurdson, K., & Kamionkowski, M., 2006, *Phys. Rev. Lett.* 97, 031301
- Pryor, C. 1992, *Morphological and Physical Classification of Galaxies*, 178, 163
- Sheth, R. K. 1995, *MNRAS*, 276, 796
- Sheth, R. K. 1996, *MNRAS*, 281, 1277
- Sheth, R. K. 1998, *MNRAS*, 300, 1057
- Sheth, R. K., & Lemson, G. 1999, *MNRAS*, 305, 946
- Sheth, R. K., & Tormen, G. 1999, *MNRAS*, 308, 119
- Sheth, R. K., Mo, H. J., & Tormen, G. 2001, *MNRAS*, 323, 1
- Sheth, R. K., & Tormen, G. 2002, *MNRAS*, 329, 61
- Sheth, R. K. 2003, *MNRAS*, 345, 1200
- Sheth, R. K., & Tormen, G. 2004, *MNRAS*, 349, 1464
- Somerville, R. S., & Kolatt, T. S. 1999, *MNRAS*, 305, 1
- Somerville, R. S., Lemson, G., Kolatt, T. S., & Dekel, A. 2000, *MNRAS*, 316, 479
- Somerville, R. S. 2002, *ApJL*, 572, L23
- Spergel, D. N., et al. 2007, *ApJS*, 170, 377
- Springel, V., Yoshida, N., & White, S. D. M. 2001, *New Astronomy*, 6, 79
- Springel, V., White, S. D. M., Tormen, G., & Kauffmann, G. 2001, *MNRAS*, 328, 726
- Springel, V. 2005, *MNRAS*, 364, 1105
- Springel, V., White, S. D. M., Jenkins, A., Frenk, C. S., Yoshida, N., Gao, L., Navarro, J., Thacker, R., Croton, D., Helly, J., and 7 coauthors, 2005, *Nat*, 435, 629
- Springel, V., White, S. D. M., Frenk, C. S., Navarro, J. F., Jenkins, A., Vogelsberger, M., Wang, J., Ludlow, A., Helmi, A. 2008, *MNRAS*, 391, 1685
- Tormen, G., Moscardini, Yoshida, 2004.
- Vale, A., & Ostriker, J. P. 2006, *MNRAS*, 371, 1173
- van den Bosch, F. C., Tormen, G., & Giocoli, C. 2005, *MNRAS*, 359, 1029
- Wilkinson, M. I., Kleyna, J. T., Evans, N. W., Gilmore, G. F., Irwin, M. J., & Grebel, E. K. 2004, *ApJL*, 611, L21
- Zentner, A. R., Berlind, A. A., Bullock, J. S., Kravtsov, A. V., & Wechsler, R. H. 2005, *ApJ*, 624, 505